Cassini Discovers a Kinematic Spiral Ring Around Saturn

S. Charnoz,[1]* C. C. Porco,[2] E. Déau,[1] A. Brahic,[1]
J. N. Spitale,[2] G. Bacques,[1] K. Baillie[1]

Since the time of the Voyager flybys of Saturn in 1980–1981, Saturn's eccentric F ring has been known to be accompanied on either side by faint strands of material. New Cassini observations show that these strands, initially interpreted as concentric ring segments, are in fact connected and form a single one-arm trailing spiral winding at least three times around Saturn. The spiral rotates around Saturn with the orbital motion of its constituent particles. This structure is likely the result of differential orbital motion stretching an initial cloud of particles scattered from the dense core of the F ring. Different scenarios of formation, implying ringlet-satellite interactions, are explored. A recently discovered moon candidate, S/2004 S6, is on an orbit that crosses the F-ring core at the intersection of the spiral with the ring, which suggests a dynamical connection between S/2004 S6 and the spiral.

Saturn's F ring has been one of the most intriguing structures around Saturn since it was first imaged by Voyager in 1980 (*1*). Its time-changing appearance and diversity of transient embedded structures (e.g. "clumps," "braids," "kinks," etc.), with short lifetimes on the order of several weeks, have challenged researchers for decades. High-resolution images (3 km per pixel) taken by Voyager 2 revealed the ring to be composed of a primary bright narrow ring, called the core, surrounded by dimmer strands on either side (Fig. 1). The number of strands and their shapes seemed to vary with time and longitude of observation. However, the Voyager images revealed only local portions of the F ring; it was not imaged over 360° with high resolution. Different models were proposed that suggested that the strands are eccentric and concentric ring segments extending ~45° in longitude (*2*), or are alternatively a collection of clumps of material orbiting near the F-ring core (*3*).

High-resolution "movie" sequences obtained by the Cassini Narrow Angle Camera (NAC) in November 2004, April 2005, and May 2005, covering 360° of orbital motion of the F-ring material, reveal that the strands are each one coil of a one-armed spiral that crosses the core of the main ring. In these sequences, the camera's field of view was positioned at the ansa of the F ring and the camera was shuttered with a frequency sufficiently high (table S1) to capture all the material passing through the field of view. The ring material was observed as if by scrolling with a fixed observation window in a Saturn-centered inertial frame for a full orbital period of 15 hours. We observed the ring this way three times, centered at 160°, 49°, and 135° longitude in November, April, and May, respectively. Note that in such a sequence, the eccentric nature of the F ring is not evident: Its precession rate is only 2.7° per day (*4*), and throughout these fixed-longitude sequences its orbital distance from Saturn changes little.

Data processing. These observations produced high-resolution (<10 km per pixel), nearly 360° "movie maps" of Saturn's F ring. A movie map is a mosaic of images showing one portion of the ring in Saturn's inertial frame at different consecutive epochs (whereas a "snapshot map" would be a mosaic showing the full ring at 360° but at a single epoch). The images' absolute positions were determined by measuring the position of either the A ring edge or stars in the images as fiducial features. The navigation was deemed accurate because of the proper coincidence (within 2 pixels) of the predicted and observed positions of satellites such as Prometheus and Pandora (*5*). All images were then reprojected and reconstructed so that the eccentric F-ring core became a line of constant radius centered on the core. This transformation preserves the scale of structures. These reconstructed maps were finally assembled into a continuous mosaic, with image time increasing to the left (Fig. 2). Assuming a constant F-ring mean motion of 582.05° per day (*6*), the time elapsed from the beginning of the observation was converted into a longitude system corotating with the motion of the F-ring particles, such that orbital longitude increases to the right. The origin of longitude is the intersection of the ascending node of Saturn's ring plane on Earth's equator at the J2000 epoch. For direct comparison, all maps have been precessed to the epoch of 1 July 2004 18:00:00 UTC. Each map is duplicated and repeated across 2 × 360° of longitude to aid examination of the azimuthal structure of the ring (Fig. 2) (fig. S1).

A spiral structure revealed. The F-ring core appears as a bright horizontal ribbon at the center of the three maps, with an irregular shape usually believed to be the consequence of the gravitational influence of nearby satellites (*5*, *7*–*9*). The strands appear as dim inclined features above and below the F-ring core. Three characteristics are striking: (i) The strands appear differently in the three maps, which suggests either a rapid evolution or a changing shape with the longitude of the observation; (ii) they do not appear as concentric ringlets (in which case they would be horizontal and parallel to the F ring) but rather connect to each other at 0° and 360°, suggesting a spiral structure (see table S1 for starting and ending longitude of each sequence of observation); and (iii) they seem to cross the core between 0° and 100° longitude.

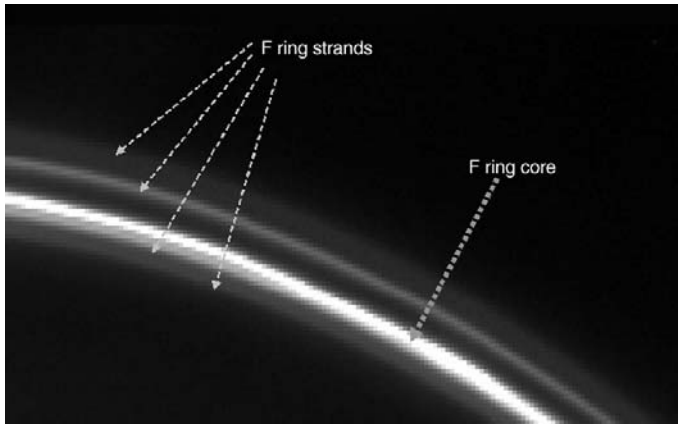

Fig. 1. The F ring as seen by Cassini on 15 November 2004, with ~35° of longitudinal extension and radial resolution of ~27 km per pixel. This image is located at 100° corotating longitude in the November map (Fig. 2).

[1]Astrophysique Interactions Multi-échelles (CEA/Université Paris 7/CNRS), DSM/DAPNIA/SAp, CEA Saclay, 91191 Gif-sur-Yvette, France. [2]Cassini Imaging Central Laboratory for Operations (CICLOPS), Space Science Institute, 4750 Walnut Street, Suite 205, Boulder, CO 80301, USA.

*To whom correspondence should be addressed. E-mail: charnoz@cea.fr

In the November maps, two strands separated by ~200 km are visible above (outside) the core and two other strands below (inside) the core, with radial separation of ~100 km. The upper strands extend longitudinally over ~750° with a full radial extension of ~500 km. Lower strands have a comparable azimuthal extension and a radial extension of 300 km. In the April and May mosaics, the strands above the core are more tightly wound with similar radial extensions (300 km), azimuthal extensions (~800°), and radial separations (~80 km), whereas strands below the core look more widely spread (500 km). All values may be inaccurate by 10% to 20% because of the diffuse nature the structure. The strands seem to cross the core around longitude 0° in November and 100° in April and May. In the latter maps, with better resolution, the core is severely distorted at this location, which suggests a real physical connection with the strands and not a simple visual superposition of two separated objects. Note also that the crossing region has an extension of 50° to 100° longitude and that several arms seem to originate from this point. This may suggest the presence of some periodic production mechanism at work. Wavy patterns are also visible; they could be real structures, or they may be artifacts attributable to an inaccuracy in the spacecraft position or in the orbital plane of the strands, inducing absolute radial displacement about ±50 km. However, this is a large-scale effect that does not affect relative distances and cannot explain why the strands appear physically connected. In addition, the continuity of brightness of the strands over their full extension implies that they are indeed a single object.

A rotating spiral. Examination of the movie maps also reveals the kinematics of the spiral structure: The overall pattern is not fixed in the inertial frame of Saturn, nor is it rotating with the precession rate of the F ring. The fact that the radial position of the strands changes with time implies that the strands are moving in Saturn's inertial frame. The rotation period of the spiral should be close to the F ring's orbital period in order to explain the reconnection of the arm with itself exactly after one F-ring orbital period (at 210° longitude in the November map). Strong similarities between the relative position of the spiral arm with respect to the F-ring core in April and in May strengthen this conclusion. Note that a simple fixed eccentric ring would not appear like this, because a piece of elliptical ring observed at the same inertial longitude always appears with the same radius. A precessing elliptical ring could explain the observations. However, at the distance of the F ring, the precession rate (2.7° per day) can only account for a radial shift of 3 to 4 km, much less than the observed 300-km radial extent of strands.

In an attempt to understand the origin of this structure, we have examined the idea that the spiral form derives from simple orbital motion (Keplerian) shear such that particles closer to the planet have larger orbital speed. Particles orbiting at different distances from Saturn have different orbital speeds according to the law $\omega(r) = (GM_p/r^3)^{1/2}$ (without considering planetary oblateness), where ω is angular speed, G is the gravitational constant, M_p is the mass of Saturn, and r is the distance to Saturn. So if, by some mechanism, a collection of particles has been scattered from a narrow ring into a cloud with Δr radial extent, it will be sheared by Keplerian motion over an angular distance α in a time $T = 2\alpha r/3\omega\Delta r$ into the shape of a trailing spiral. From the April and May observations, we measure $\Delta r \sim$ 300 km and $\alpha \sim 800°$, giving $T \sim 1.2$ years. The observed spiral might have been first generated around the beginning of 2004 (also consistent with November observations). If Keplerian shear is really the key mechanism that drives the evolution of these structures, this time scale is a strong constraint, because shear alone causes the number of arms within a fixed radial width to increase at a rate of one new arm every ~190 days. This is roughly what is observed above the ring core when comparing April and November maps (separated by 149 days) and November and May maps (separated by 170 days). However, the lifetime of a spiral structure is limited; as the material is spread over more and more arms, brightness should decrease linearly with

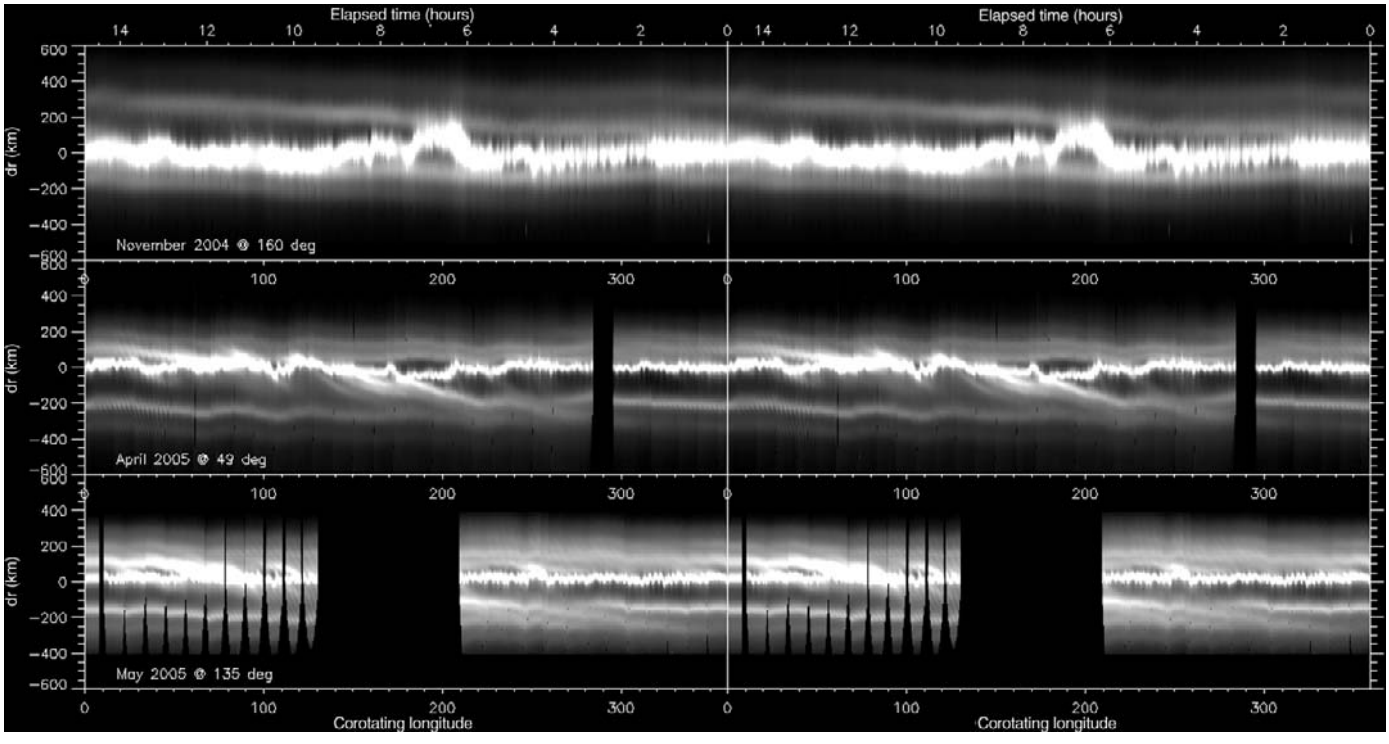

Fig. 2. Maps of the F ring in November (upper) with radial resolution of ~27 km per pixel, April (middle) with radial resolution of ~6.5 km per pixel, and May (bottom) with radial resolution of ~5 km per pixel. All maps are precessed to the epoch 1 July 2004 18:00:00, using a mean motion of 582.05° per day. The *x* axis is the corotating longitude; the *y* axis is the distance from the F-ring core in kilometers. The F-ring core is the bright horizontal line in the center of all maps. The strands appear as dimmer inclined lines below and above the core. Faint structures may be more visible in fig. S1.

time, and the structure might be expected to fade away.

What mechanism might scatter particles out of the F-ring core? If the spiral is made of micrometer-sized particles, what would regenerate and maintain it against radiative effects, such as Poynting-Robertson drag or light pressure (*10*), that sweep small particles into the planet? The F-ring strands have been observed since the Voyager epoch, so a regeneration mechanism is required. Impacts with meteoroids or micrometer-sized particles released by Enceladus (*10*–*13*) are not implausible, but these are intrinsically random events that likely cannot explain the constant regeneration of a coherent structure like the observed spiral. Because such a temporally limited data set does not allow us to dismiss random impacts, we instead investigated the scenario of a close interaction between the F-ring core and a satellite on an eccentric orbit. We considered this scenario for two reasons: (i) Satellite-ringlet interactions are known to play a major role in the dynamical evolution of ringlets (*7*, *8*, *14*), and (ii) a satellite on an eccentric orbit can interact periodically with a nearby ringlet, constantly generating new structures longitudinally spaced by $3\pi\Delta a/a$ [where a and $a + \Delta a$ are the semimajor axes of the F-ring core and of the satellite, respectively (*15*)]. In addition to Prometheus and Pandora, the F ring has long been suspected to shelter a population of small unseen moons (*16*, *17*).

A simple numerical model. Simulations of a satellite interacting with the F-ring strands have been performed for Prometheus in the past (*8*) and more recently (*9*) over a few orbital periods. Our simulations extended over 2000 orbital periods to follow the Keplerian shear of particles in a narrow ring intersected every orbital period by a massive satellite. Including the effect of Saturn's oblateness, we computed the trajectories of 10^4 test particles in orbit around Saturn, gathered into a longitudinally limited ringlet and perturbed by a satellite. At the beginning, the particles were given the same orbital parameters as the F-ring core (*4*), with semimajor axis at 140,223 km. To test the code, we reproduced the formation of drapes in the F ring as seen on 1 July 2004 in earlier Cassini images (fig. S2) (*9*). To follow the interaction in detail, we gathered all particles at the beginning of the simulation in a small segment extending 0.5° in longitude and on a trajectory intersecting the satellite's orbit. Because we wanted to simulate a strong interaction to test the basic mechanisms of the ring-satellite scenario, the satellite's semimajor axis was set at 139,600 km (120 km closer to the F ring than today's Prometheus), its eccentricity at 0.0023, and its orbit anti-aligned with the F ring's so that it crosses the ring at the ring's pericenter (the location where the ring is closest to Saturn). In such a simulation, the mass of the required satellite is critical: After a single encounter, a satellite scatters neighboring particles over a distance of a few Hill's radii. The Hill's radius is the typical distance of gravitational influence of a satellite, given by $a(M_s/3M_p)^{1/3}$, where a is the satellite's semimajor axis, M_p is Saturn's mass, and M_s is the satellite's mass (*18*). Therefore, in these simulations the satellite's mass was set to 2×10^{17} kg (comparable to that of Prometheus) in order to scatter particles over the radial extent of the spiral (~300 km). Whereas the simulated satellite's characteristics were similar to those of Prometheus, the latter is not currently on an intersecting orbit with the F-ring core. However, in 2009 its orbit will be anti-aligned with the orbit of the F ring because of the precession induced by Saturn's oblateness (*2*, *8*).

Immediately after the simulated satellite encounter (Fig. 3A) (fig. S3), particles are scattered out of the ringlet over ~300 km, in agreement with the prediction. They are separated into three groups because in these simulations the satellite crosses the ring twice: before and after its apocenter (the place where the body reaches its maximum distance from Saturn). Those groups are subsequently stretched and sheared by Keplerian motion. After 300 orbits (~6 months), they have differentially spread over 360°, producing a trailing spiral structure. After 700 orbits of evolution (~1.2 years), the spiral structure is clear and extends below and above the original location of the ring (Fig. 3B). It winds around the planet about three times. The arms are discontinuous because of the original division into three groups.

To illustrate the motion of the spiral, Fig. 3C shows the configuration of particles just half a period after Fig. 3A. Although the overall shape is the same, the radial structure of the spiral has changed. Inspection of the particles' orbital elements reveals that the shape and orientation of their orbits remain very close to those of the original ring. The greatest change occurring from the interaction with the satellite is the alteration of the particles' semimajor axes by about ±200 km (eccentricities vary by about ±0.001 only). As a consequence, on short time scales the spiral is carried along by the particles' orbital motions. Moreover, because the particles retain values of eccentricity and apse locations close to that of the F ring, the arms will be more separated near the apocenter of the F ring than near the pericenter. This effect is clearly visible in Fig. 3, B and C. On longer time scales (~1800 orbits, 3 years) the spiral structure will disappear because of multiple reinteractions with the satellite that randomly scatter the already scattered particles. Note also that the strands remain parallel with the F-ring core as a result of initial conditions (this was a major issue in previous work on the F-ring strands) (*2*). Numerous other configurations were investigated by varying the mass and location of the satellite or assuming that particles are scattered from the

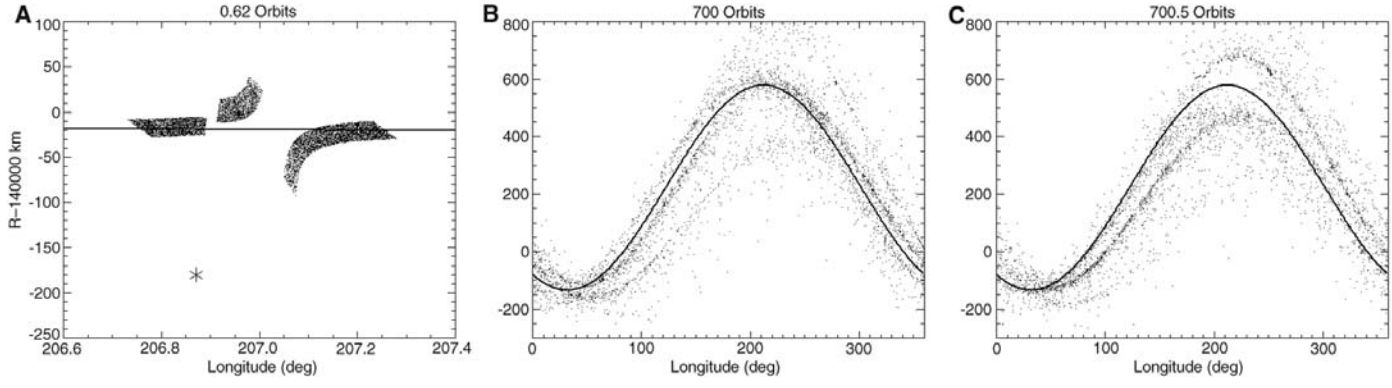

Fig. 3. Simulation of a piece of ringlet, with 0.5° starting extension, interacting with a satellite on a crossing orbit at three different epochs. The *x* and *y* axes are the longitude and distance to Saturn, respectively. Particles are represented by dots; the perturbing satellite is denoted by an asterisk. The center of the F-ring core is represented by the solid back curve. (**A**) Just after the close interaction with the satellite. (**B**) 700 orbits after the interaction; the scattered particles have spread at 360° around the planet and the material is now organized as a spiral arms winding three or four times. (**C**) Same as previous, but half an orbit later to reveal the rotation of the spiral. The satellite's apocenter is located at 65° longitude. See fig. S3 for a color version of the plot.

strands themselves. All such simulations show that a smaller satellite (with radius of a few kilometers) is not massive enough to gravitationally scatter material over 300 km, and that the source of the particles must be the F-ring core itself in order to reproduce both exterior and interior spirals, as seen in the images.

Reproducing observations. We simulated the conditions of Cassini observations to examine and compare our model results with the movie maps. Three observing windows were defined in Saturn's inertial frame (each extending 30° longitude) to reproduce the November, April, and May conditions of observation. We found qualitative agreement for the November and April maps (Fig. 4, A and B), whereas we were less successful for the May map (Fig. 4C), in which the spiral seemed more tightly wound than in the simulation, perhaps because of the great simplicity of this model. An interesting aspect of these synthetic observations is that they show how different the spiral may appear when observed at different longitudes: As a result of its complex longitudinal and radial structure (Fig. 3, B and C), the spiral may appear with varying numbers of branches with different radial locations, depending on the longitude of observation (Fig. 4).

These results clearly show that a massive satellite, after a single interaction, can scatter particles efficiently from a narrow ring, after which orbital shear can then draw them into a rotating spiral. However, our simulations followed only a 0.5°-wide portion of the F ring encountering the satellite. The effect of the satellite over the full ring is not clear because multiple mechanisms are at work with opposite effects. On one hand, the lifetime of a single spiral arm is limited by repeated encounters with the satellite and by the natural fading away of the structure as a result of Keplerian shear. On the other hand, multiple encounters of the same satellite with the F-ring core would trigger the formation of additional spirals—one new spiral for every orbital period of the satellite—longitudinally spaced by $3\pi\Delta a/a$ (in radians). Whether or not successive spirals merge together (to form a featureless cloud) or enhance each other would depend on the orbital separation of the satellite and ring: If successive spirals have very small longitudinal separations, as they would in the case of a perturbing satellite with a semimajor axis very close to the F ring's, then they could combine into a single bright arm. Complicating things further, new spirals may differ in brightness because the F-ring core exhibits strong density variations, and at some longitudes, passage through the ring may not scatter much material. The combination of all these effects is obviously difficult to anticipate, and a full simulation is not possible because of computer limitations.

The role of a new satellite. The recent Cassini discovery of objects in the F-ring region (*5*, *19*) has proved promising. One of them, S/2004 S6, is relatively long-lived (more than 1 year) and may be a moon or an extended clump. It is on an eccentric, inclined orbit that crosses the F ring at 16°, 86°, and 96° in the November, April, and May maps, respectively, matching well the location where the spiral intersects the F-ring core. Its radial excursions beyond the ring, both interior and exterior, are several hundred kilometers, comparable to the radial extent of the spiral. These coincidences strongly suggest that S6 may be involved in the formation of the spiral. S/2004 S6 is much smaller than Prometheus and so cannot gravitationally scatter particles over 300 km. However, it may be possible that S6 drags particles out of the ring via nongravitational effects such as physical rebound at the satellite's surface. The magnitude of a perturbation on a particle's orbit may be roughly measured by the variation of its orbital speed, Δv. To scatter particles radially from the F-ring core over 300 km requires a Δv in the range of 25 m/s (from simple comparison of orbital velocities). Gravitational scattering by tiny S6 would give a Δv of only ~2 m/s, well below the required value (assuming a mass density of 0.8 g/cm^3 and a diameter of 5 km). However, on its present orbit, S6 encounters the F ring with a relative speed of ~30 m/s. Particles suffering inelastic collisions on its surface may undergo a Δv comparable to, although lower than, their impact velocity, which is roughly what is needed to scatter them over 300 km. Note also that S6 likely has a very low density, comparable to that of other ring-region moons (*5*), and may not be massive enough to accrete particles colliding with it because of its very low escape velocity (~2 m/s). In addition, S6 is very close to the F-ring region [$3\pi\Delta a/a \sim 0.34°$ (*19*)], and it may be possible that its repeated passages through the ring's core enhance the spiral (see above). This very rough calculation needs further investigation with a detailed model.

Whatever the mechanism that removes particles from the F-ring core, the Keplerian shear of scattered particles supplies a natural explanation for the variations in the appearance and in the number of arms observed as a function of longitude and time. Other effects, such as radiative forces or plasma drag, may in principle affect the particles' orbits. Whereas the core of the F ring seems to be made of big and small particles (*4*, *11*), the surrounding region seems populated by micrometer-sized particles (*12*, *20*) that will be sensitive to radiation effects (*10*). For the moment, no dynamical model of the F ring including radiative effects has been published. However, radiative effects act on time scales that are long relative to the observed evolution time of the spiral and are not likely to be important.

This interpretation of the F-ring strands should be compared to two previous investigations of the F ring based on Voyager images (*2*, *3*) with partial azimuthal coverage. In the first study, strands are envisioned as four nonintersecting and concentric arc-like rings extending ~45° in longitude with orbits aligned with the F-ring core. They were so described because of the changing number of visible strands in images. In the spiral model, the changing number of visible strands

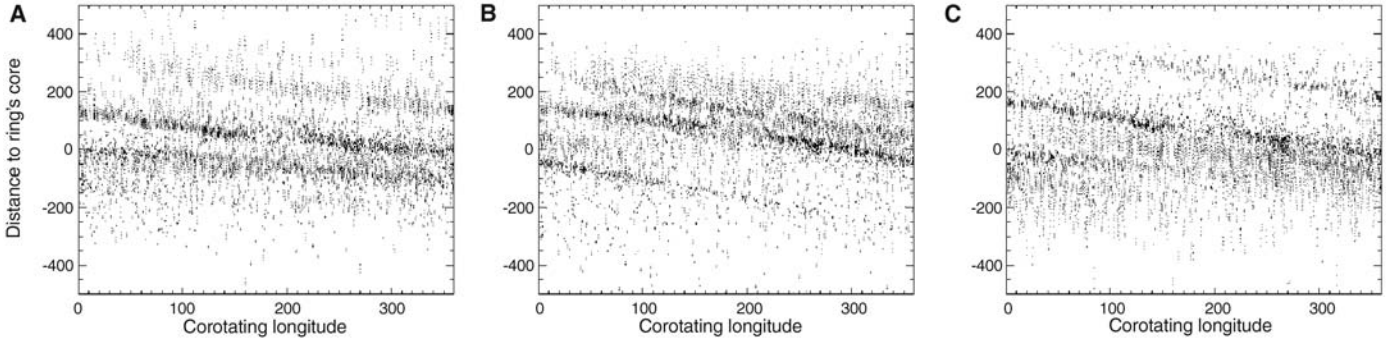

Fig. 4. The simulated spiral as if seen by Cassini. The spiral (Fig. 3) is observed passing through a constant observation window in Saturn's inertial frame during one orbital period. The results from three different observation windows are shown (at longitudes 300°, 189°, and 275° in Fig. 3, from left to right) to reproduce the conditions of observation in (**A**) November 2004, (**B**) April 2005, and (**C**) May 2005. The *x* axis is longitude; the *y* axis is the distance to the ring's core (in kilometers).

is a natural consequence of the longitude of observation, and the spreading by Keplerian shear explains also why they all appear concentric. In the second study, several clumps were tracked around Saturn, indicating a full 90-km range in semimajor axes (with a standard deviation of 45 km). The observations reported here show that the strands, organized as a rotating spiral, have a wider range of semimajor axes (300 km); however, it may be possible that the tracked clumps were only the brightest ones, naturally located closer to the core in the spiral model.

By the end of 2009, Prometheus and the F ring will be in a close-encounter configuration because of the precession of their orbits resulting from Saturn's oblateness (*2*, *8*). It is very probable that additional spirals will then be created by Prometheus and could be observed in an extended Cassini mission.

References and Notes

1. B. A. Smith *et al.*, *Science* **212**, 163 (1981).
2. C. D. Murray, M. K. Gordon, S. M. G. Winter, *Icarus* **129**, 304 (1997).
3. M. R. Showalter, *Icarus* **171**, 356 (2004).
4. A. S. Bosh, C. B. Olkin, R. G. French, P. D. Nicholson, *Icarus* **157**, 57 (2002).
5. C. C. Porco *et al.*, *Science* **307**, 1226 (2005).
6. P. D. Nicholson *et al.*, *Science* **272**, 509 (1996).
7. M. R. Showalter, J. A. Burns, *Icarus* **52**, 526 (1982).
8. C. D. Murray, S. M. G. Winter, *Nature* **380**, 139 (1996).
9. C. D. Murray *et al.*, *Nature* **437**, 1326 (2005).
10. J. A. Burns, D. P. Hamilton, M. R. Showalter, in *Interplanetary Dust*, E. Grün, B. A. S. Gustafson, S. F. Dermott, H. Fechtig, Eds. (Springer-Verlag, Berlin, 2001), pp. 641–725.
11. M. R. Showalter, *Science* **282**, 1099 (1998).
12. M. R. Showalter, J. B. Pollack, M. E. Ockert, L. Doyle, J. B. Dalton, *Icarus* **100**, 394 (1992).
13. D. P. Hamilton, J. A. Burns, *Nature* **365**, 498 (1993).
14. M. C. Lewis, G. R. Stewart, *Astron. J.* **120**, 3295 (2000).
15. S. F. Dermott, *Nature* **290**, 454 (1981).
16. R. A. Kolvoord, J. A. Burns, M. R. Showalter, *Nature* **345**, 695 (1990).
17. J. Hänninen, *Icarus* **103**, 104 (1993).
18. C. C. Porco *et al.*, *IAU Circ. 8432*, 1 (2004).
19. J. N. Spitale, unpublished data.
20. F. Poulet, B. Sicardy, P. D. Nicholson, E. Karkoschka, J. Caldwell, *Icarus* **144**, 135 (2000).

21. We thank H. Throop, J. Cuzzi, J. Decriem, C. Ferrari, M. Hedman, C. Murray, P. Nicholson, M. Tiscareno, and three anonymous referees for useful comments and discussions. We also acknowledge the work of the CICLOPS operations group in making the observations described here possible.

Supporting Online Material

www.sciencemag.org/cgi/content/full/310/5752/1300/DC1
Table S1
Figs. S1 to S3

26 August 2005; accepted 19 October 2005
10.1126/science.1119387

REPORTS

Encoding Electronic Properties by Synthesis of Axial Modulation-Doped Silicon Nanowires

Chen Yang,[1]* Zhaohui Zhong,[1]* Charles M. Lieber[1,2]†

We describe the successful synthesis of modulation-doped silicon nanowires by achieving pure axial elongation without radial overcoating during the growth process. Scanning gate microscopy shows that the key properties of the modulated structures—including the number, size, and period of the differentially doped regions—are defined in a controllable manner during synthesis, and moreover, that feature sizes to less than 50 nanometers are possible. Electronic devices fabricated with designed modulation-doped nanowire structures demonstrate their potential for lithography-independent address decoders and tunable, coupled quantum dots in which changes in electronic properties are encoded by synthesis rather than created by conventional lithography-based techniques.

A wide range of nanoscale electronic and photonic devices have been made with carbon nanotube and nanowire functional elements (*1*–*4*). Although the nanomaterials are important for achieving observed functional properties in these nanodevices, many of the most critical features have been defined with the use of similar lithographic approaches that drive and ultimately limit the planar semiconductor industry. The current dependence on lithography thus could reduce advantages of these nanoscale elements in proposed applications and suggests that nonlithographic approaches for encoding key features or information are needed.

Modulation of the composition has been demonstrated recently in relatively simple nanorod and nanowire structures to yield functional structures (*5*–*8*). For example, gold grown on the tips of cadmium selenide nanorods provides specific points for self-assembly and electrical contact (*5*). Modulation of the dopant or composition of nanowires during synthesis also has been used to define functional *p*-type/*n*-type diodes (*6*) and single quantum dots (*8*). These studies show the potential for synthesis to define function without lithography, yet the level of information and function encoded in the materials has been very limited. We now describe selective dopant modulation during the growth of silicon nanowires with essentially complete control over the size, spacing, and number of modulated regions.

Applications of nanowires in conventional electronics could be facilitated by using synthesis to define the aspects of transistors that are currently enabled by lithographic and ion-beam processing, such as feature uniformity and controlled doping. For example, the high sensitivity of carbon nanotubes to adsorbed gases and solid coatings, along with lithographic patterning, has been exploited in transistor structures (*9*, *10*). Greater ease of circuit assembly could be afforded by the ability to create semiconductor nanowires that are uniform in shape and that can be doped selectively along their length, in that the formation of regions with different electronic properties would be intrinsic to nanowire synthesis and would not require intermediate lithographic patterning and/or electrical contacts. Many of the wiring steps normally created by lithography can be encoded by varying the doping sequence of the nanowires so that the only postfabrication lithographic steps would be those involved in making external input and output contacts to individual nanowires.

Synthesis of dopant-modulated nanowire structures in which function can be predicted on the basis of the encoded axial sequence of doping is challenging: It requires effectively pure axial or one-dimensional (1D) growth without simultaneous radial or 2D growth (Fig. 1A), because even a few atomic layers of dopant deposited on the surface of a nanowire can dominate its overall electronic properties (*11*). In the metal nanocluster-catalyzed vapor-liquid-solid growth process (*3*–*5*), which has been widely used to prepare nanowires, the dopant must be added exclusively at the nanocluster catalyst without reaction and deposition at the much larger area of the exposed solid

[1]Department of Chemistry and Chemical Biology, [2]Division of Engineering and Applied Sciences, Harvard University, Cambridge, MA 02138, USA.

*These authors contributed equally to this work.
†To whom correspondence should be addressed. E-mail: cml@cmliris.harvard.edu